HEFAT2011
8th International Conference on Heat Transfer, Fluid Mechanics and Thermodynamics
11 – 13 July 2011
Le Meridien, Mauritius

EFFECT OF THE FLOW LEADING SLATS OBLIQUITY ON THE THERMAL PERFORMANCE OF AIR-COOLED CONDENSERS IN A POWER PLANT

Yang L. J.*, Du X. Z., and Yang Y. P.
*Author for correspondence
School of Energy Power and Mechanical Engineering,
North China Electric Power University,
Beijing, 102206,
China
E-mail: yanglj@ncepu.edu.cn

ABSTRACT

Ambient winds may bring on poor fan performance and deteriorated heat rejection of the air-cooled condensers in a power plant. The disadvantageous wind impacts can be weakened thanks to the flow field leading of the wind. By introducing a radiator model to the fin-tube bundles, the air-side fluid and heat flow in air-cooled condensers with a flow guiding device in a representative 2×600MW direct dry cooling power plant are modeled and calculated. The flow rate and heat rejection of the individual condenser cells and the air-cooled condensers with flow guiding devices at different slat obliquities are obtained and compared. The results show that the flow rate and heat rejection of the air-cooled condensers both increase owing to the setup of the flow guiding device. The low flow guiding slats obliquity is superior to the high one for the thermo-flow performances. For the upwind condenser cells, the flow and heat transfer rates vary widely due to the flow field leading of the ambient winds by the flow guiding device especially at the lowered obliquity. It can be of use for the optimal design and operation of air-cooled condensers in a power plant.

INTRODUCTION

With increased focus upon water conservation, combined with continued concern over the environmental effects of both once-through and evaporative cooling, the application of air-cooled condensers (ACCs) to power plants condenser heat rejection is expected to increase [1, 2]. The ambient air is impelled by the fans to flow through the finned tube bundles of ACCs, removing the thermal duty of the exhaust steam from a turbine. Ambient wind is considered to be one of the key issues for the ACC performance.

Many studies have found that air-cooled condensers work fairly bad in a wide range of specific climate, especially with large wind speeds and unfavourable wind directions. By using computational fluid dynamics (CFD) methods, Duvenhage and Kroger [3] investigated the effects of wind on the fan performance and recirculation in air-cooled condensers and found that cross wind significantly reduces the air flow rate in the upwind condenser cells, and that the wind along the longitudinal axis cause increased hot plume recirculation. The trend is similar to that obtained from the experimental measurements by Cooling Tower Institute of America. van Rooyen and Kroger [4] numerically studied the air flow field about and through a particular air-cooled condenser, in which the performance of the fan is modelled with the aid of the numerical approach - actuator disc model. It is found that the reduction in fan performance is the main reason for the poor ACC performance while recirculation of hot plume air only reduces performance by a small amount. Hotchkiss et al. [5] studied the effects of the cross flow on the performance of the axial flow fans in air-cooled condensers by using actuator disk fan model. The investigation revealed that the adverse effect of the off-axis inflow on fan static pressure rise was attributed to two factors, increased kinetic energy per unit volume at the fan exit and greater dissipation through the fan itself. Off-axis inflow was found to affect fan-blade loading characteristics with implications for blade fatigue. By also using actuator disk model, Meyer [6] numerically investigated the effect of the inlet flow distortions and found that the inlet flow losses of the periphery fan are dominated by the flow separation occurring around the lip of the fan inlet section. These flow losses can be reduced by the installation of a walkway at the edge of the fan platform or by the removal of the periphery fan inlet section. Duvenhage et al. [7] also numerically and experimentally studied fan performance in air-cooled condensers during inlet flow distortions. By experimental measurements, Meyer and Kroger [8, 9] investigated the effects of fan, heat exchanger characteristics and the plenum chamber geometry on the flow losses of air-cooled condensers. Bredell et al. [10] numerically investigated the effect of inlet flow distortions on the flow rate through the fans, and considered the volumetric effectiveness of

two different types of axial flow fans at different platform heights. Their results also showed that the addition of a walkway can significantly increase the flow rate through the fans near the edge of the fan platform. Gu et al. [11] conducted a wind tunnel experiment of the air-cooled condensers at a large power plant to investigate the recirculation of hot exhaust air and its dependence on wind directions. They found that the wind speed and direction as well as the height of ACC platform have a significant impact on the recirculation..

The aforementioned research all show that the wind effects, which include issues such as fan performance impacts, plume recirculation effects, tube bundle exhaust air flows, represent a major challenge associated with the ACC operation. In order to weaken the adverse impacts of ambient winds on the ACC performance, various measures have been proposed [12-14], among which an effective method adding deflecting plates under the air-cooled condenser platform was presented. In this paper, the flow field leading of ambient winds that may lessen the adverse impacts of winds in a representative 2×600MW power plant is investigated. The emphasis is placed on the influence of the flow leading slats obliquity on the thermo-flow characteristics of the ACCs and the individual condenser cells. It can be of use for the optimal design and operation of direct dry cooling system in a power plant.

NOMENCLATURE

C	[-]	*k-ε model constant*
e	[J/kg]	Specific internal energy
f_n	[-]	Polynomial coefficient of the pressure rise of the fan
g	[m/s^2]	Gravitational acceleration
G	[m^2/s^2]	Turbulence kinetic energy generation
g_n	[-]	Polynomial coefficient of the tangential velocity of the fan
h	[W/m^{2}k]	Air-side convection heat transfer coefficient
h_n	[-]	Polynomial coefficient of convection heat transfer coefficient
h_e	[J/kg]	Specific enthalpy
k	[m^2/s^2]	Turbulence kinetic energy
k_L	[-]	Non-dimensional loss coefficient
m	[-]	Exponent of the wind speed in power-law equation
p	[Pa]	Pressure
q	[W/m^2]	Heat flux
Q_v	[m^3/s]	Volumetric flow rate
r	[m]	Radial distance from the fan center
r_n	[-]	Polynomial coefficient of non-dimensional loss coefficient
s_h	[W/m^3]	Volumetric heat source
T	[K]	Temperature
u_i	[m/s]	Velocity
v	[m/s]	Normal component of velocity
x_i	[m]	Cartesian coordinate
z	[m]	Height above the ground

Greek symbols

β	[°]	Flow leading slats obliquity
ρ	[kg/m^3]	Air density
μ	[kg/m s]	Air dynamic viscosity
ν	[m^2/s]	Air kinetic viscosity
λ	[W/mK]	Air thermal conductivity
τ	[J/m^3]	Stress tensor
σ	[-]	Turbulent Prandtl number
ε	[m^2/s^3]	Turbulence kinetic energy dissipation rate
Φ	[W]	Heat rejection

Subscripts

w	Wind
a	Air

COMPUTATIONAL MODELS

The layout of the ACCs with the flow guiding device (FGD) and main buildings consisting of the boiler and turbine rooms and chimney in a typical 2×600MW direct dry cooling power plant is schematically shown in Figure 1. An air-cooled condenser consists of an array of the condenser cells. For each condenser cell, the finned tube bundles are arranged in the form of an A-frame fitted with an axial flow fan below. There are two ACCs in this power plant, with each ACC having 56 (7×8) condenser cells.

Figure 2 gives the schematic of the flow guiding device configurations. The flow guiding device is installed below the platform. It consists of 3 layers smooth flat slats in four sides as shown in Figure 2 (a). The dimensions of the FGD are shown in Figure 2 (b). The obliquity β of the FGD slats is taken to be 30°, 45° and 60° to investigate the influence of the obliquity on the thermo-flow performances of the ACCs in this paper. In order to prevent unrealistic flow effects caused by the flow domain boundaries from affecting the flow near the region of interest, the physical domain should be taken large enough. Figure 3 gives the computational domain with the size of $2240\text{m} \times 2240\text{m} \times 720\text{m}$ ($x \times y \times z$). Thanks to the geometric symmetry of the ACCs and main buildings, only half of the wind directions are considered. Five representative wind direction angles of interest, -90° (*y* direction), -45°, 0° (*-x* direction), 45°, 90° (*-y* direction), are schematically indicated in Figure 3. The computational meshes are generated with commercial software Gambit using multi-block hybrid approach. For the central domain with the ACCs and main buildings, the tetrahedral unstructured grid is used. For other zones, hexahedral structured grid is used. Grids consisting of about 1,420,500, 2,089,800, and 2,650,000 cells are tested for the ACCs without FGD at the wind speed of 3m/s and direction angle of 0°. The overall volumetric flow rate of the cooling air in the two ACCs is observed to vary by only about 0.9% between the two highest grid density solutions. So the final grids number used is about 2,089,800 for the simulation of the ACCs without FGD. The grid independence check is also made for the performance simulation of the ACCs with FGD. The total counts of the volume meshes for the ACCs with FGDs at three obliquities are 2,337,700, 2,346,500 and 2,339,200 respectively.

The fluid and heat flow of the cooling air in air-cooled condensers is a multi-scale phenomenon, simplifications for the tube bundles and axial flow fans are taken into consideration. A lumped-parameter radiator model is used to deal with the fin-tube bundles and the fan is simplified as a pressure jump surface in this paper.

In the radiator model, the pressure drop Δp varies with the normal component of the velocity v through the fin-tube bundles as follows

$$\Delta p = k_L \frac{1}{2} \rho v^2 \quad (1)$$

where ρ is the air density, k_L is the non-dimensional loss coefficient, which can be expressed as a polynomial function.

$$k_L = \sum_{n=1}^{N} r_n v^{n-1} \quad (2)$$

where r_n is the polynomial coefficient. On the basis of the experimental data of the air flowing through the wave-finned flat-tube bundles that are commonly adopted by the Single Row Condenser design of the 600MW generating unit, the polynomial coefficients are calculated and listed in Table 1.

Table 1 Polynomial coefficients that fit the pressure drop of the air flowing through the finned tube bundles.

r_1	r_2	r_3
71.68881	-31.70742	4.79819

The heat flux q from the radiator to the surrounding air is given as

$$q = h(T_s - T_{a,d}) \quad (3)$$

where T_s is the saturation temperature of the exhaust steam and can be regarded as the tube outer wall temperature if the conductive thermal resistance through the wall and the condensation thermal resistance are both neglected. $T_{a,d}$ is the air temperature downstream of the radiator. The convective heat transfer coefficient h is normally specified as a polynomial function of the normal component of velocity.

$$h = \sum_{n=1}^{N} h_n v^{n-1} \quad (4)$$

where h_n is the polynomial coefficient as given in Table 2 to match the heat transfer experimental results of the cooling air in the air-cooled condensers.

Table 2 Polynomial coefficients that fit the heat transfer experimental data.

h_1	h_2	h_3
536.993	2016.0887	-97.77205

For the fan surface, the pressure rise is generally expressed as the polynomial form of the axial velocity v of the fan.

$$\Delta p = \sum_{n=1}^{N} f_n v^{n-1} \quad (5)$$

where f_n is the polynomial coefficient. In terms of the performance curve of the typical fan adopted by the air-cooled condensers, the polynomial coefficients are obtained as shown in Table 3.

Table 3 Polynomial coefficients that fit the performance curve of the axial flow fan.

f_1	f_2	f_3	f_4	f_5
195.59557	-19.99838	3.96681	-0.56975	0.0219

Owing to the three-dimensional flow complexities caused by the fan blades, the values of the tangential and radial velocities are imposed on the fan surface to generate swirl. These velocities can be specified as the functions of the radial distance from the fan centre. In this paper, the radial velocity is neglected. The tangential velocity component u_θ can be specified by the following equation.

$$u_\theta = \sum_{n=-1}^{N} g_n r^n \quad -1 \le N \le 6 \quad (6)$$

where r is the radial distance from the fan center. g_n is the polynomial coefficient. When the geometric details of the fan blades are known, the tangential velocity at different radial distance can be obtained. The polynomial coefficients that fit the tangential velocity are listed in Table 4.

Table 4 Polynomial coefficients that fit the tangential velocity of the axial flow fan.

g_{-1}	g_0	g_1	g_2	g_3
-15.1	25.76	-11.791	4.321	-0.354

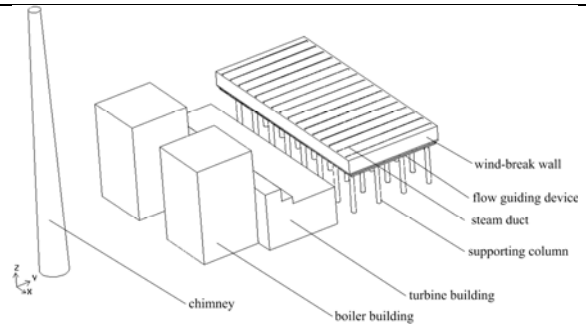

Figure 1 Schematic of the ACCs with the flow guiding device and the main buildings in a power plant.

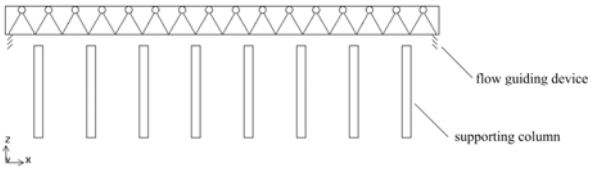

(a)

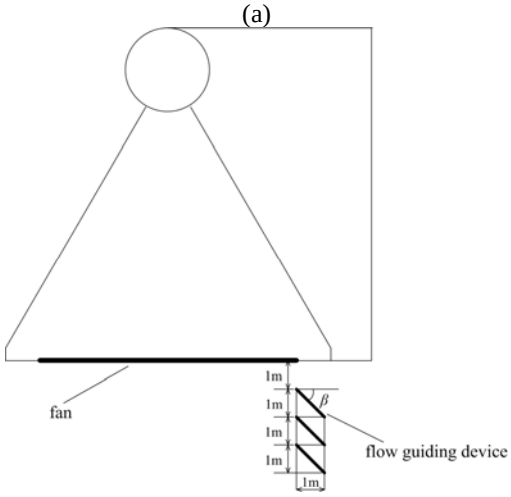

(b)

Figure 2 (a) Schematic of the flow guiding device installation, (b) Schematic of the geometric details of the flow guiding device.

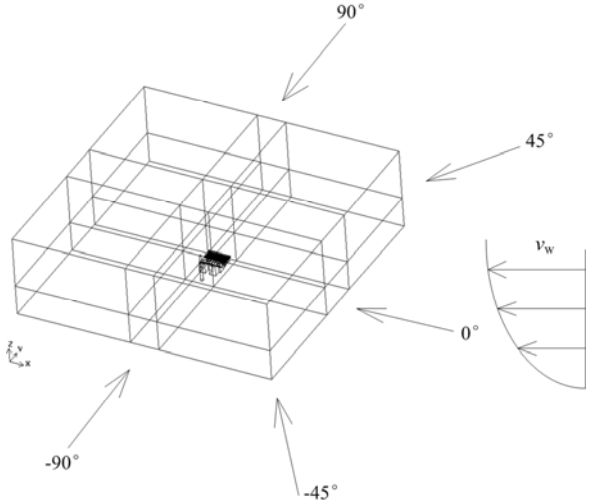

Figure 3 Computational domain and specification of the wind direction angles.

Governing Equations

The steady state governing equations on the air-side of the ACCs are as follows.

$$\frac{\partial(\rho u_i)}{\partial x_i} = 0 \qquad (7)$$

$$\frac{\partial(\rho u_i u_j)}{\partial x_j} = \frac{\partial}{\partial x_j}\left[\mu_{eff}\left(\frac{\partial u_i}{\partial x_j}+\frac{\partial u_j}{\partial x_i}\right)-\frac{2}{3}\mu_{eff}\frac{\partial u_k}{\partial x_k}\right]-\frac{\partial p}{\partial x_i}+\rho g_i + S_i$$

（i=1, 2, 3, and $i \neq j$） (8)

$$\frac{\partial}{\partial x_i}(u_i(\rho e+p)) = \frac{\partial}{\partial x_i}(\lambda_{eff}\frac{\partial T}{\partial x_i}+u_j(\tau_{ij})_{eff})+S_h \qquad (9)$$

where u_i is the velocity in the x_i direction, p is the pressure, g_i is the gravitational acceleration in the x_i direction. Due to the large scale of the A-frame of the condenser cell, the buoyancy effect is considered and the air is regarded as the incompressible idea gas. $e = h_e - \frac{p}{\rho} + \frac{u_i^2}{2}$, is the specific internal energy, h_e is the specific enthalpy. $\mu_{eff} = \mu + \mu_t$, is the effective dynamic viscosity, μ and μ_t are the dynamic viscosity and turbulent dynamic viscosity respectively. τ_{eff} is the stress tensor, λ_{eff} is the effective thermal conductivity. S_h is the heat resources, namely the heat rejection per volume of the air-cooled condenser.

The standard k-ε turbulent model is used to characterize the flow through the fin-tube bundles.

$$\frac{\partial}{\partial x_i}(\rho k u_i) = \frac{\partial}{\partial x_j}\left[\left(\mu+\frac{\mu_t}{\sigma_k}\right)\frac{\partial k}{\partial x_j}\right]+G_K+G_b-\rho\varepsilon \qquad (10)$$

$$\frac{\partial}{\partial x_i}(\rho\varepsilon u_i) = \frac{\partial}{\partial x_j}\left[\left(\mu+\frac{\mu_t}{\sigma_\varepsilon}\right)\frac{\partial \varepsilon}{\partial x_j}\right]+C_{1\varepsilon}\frac{\varepsilon}{k}(G_K+C_{3\varepsilon}G_b)-C_{2\varepsilon}\rho\frac{\varepsilon^2}{k} \qquad (11)$$

where k and ε are the turbulence kinetic energy and its rate of dissipation. σ_k and σ_ε are the turbulent Prandtl number for k and ε. G_k represents the generation of the turbulence kinetic energy due to the mean velocity gradients. G_b is the generation of the turbulence kinetic energy due to the buoyancy. The model constants have the following default values, $C_{1\varepsilon}=1.44$, $C_{2\varepsilon}=1.92$, $C_{3\varepsilon}=1$, $\sigma_k=1.0$, $\sigma_\varepsilon=1.3$.

The wind speed in the form of the power-law equation is appointed at the windward surface of the computational domain.

$$u = u_{10}(\frac{z}{10})^m \qquad (12)$$

where u_{10} is the wind speed at the height of 10m that is generally provided by the local weather office. z is the height. The exponent m is related to the roughness of the ground and the stability of the atmosphere, taken to be 0.2 in this simulation as an approximation. At the downstream surface, the outflow boundary condition is appointed. At the other surfaces, the symmetry boundary is set. The ground is assumed to be adiabatic. For the turbine and boiler buildings as well as the chimney, the constant heat flux is set at the surface according to the total heat flow rate and the corresponding surface area. The surfaces of the support column of the air-cooled condensers are given the adiabatic conditions approximately. The wall temperatures of the steam ducts are kept constant at the saturated temperature of the exhaust steam.

Numerical Methods

The Equations (7)-(11) combined with the boundary conditions are solved by the commercial finite-volume based solver Fluent 6.2. The governing equations for the momentum and energy in conservative form are discretized with the finite-volume formulation using a fully implicit first-order upwind differencing scheme. The SIMPLE algorithm is employed in the pressure-velocity coupling. A divergence-free criterion of 10^{-4} based on the scaled residual is prescribed for the computations. The parallel solver by using multiple processes that execute on different CPUs is employed due to the large numbers of the grids resulting from the model complexities.

The same computational models and solution methods have been validated in Yang's work [12], so the validation of the numerical results for the present study is omitted.

RESULTS AND DISCUSSION

The designing ambient temperature for the ACC in China is generally taken to be 15℃, so the ambient temperature of 15℃ is investigated. Three wind speeds of 3m/s, 9m/s and 15m/s are chosen to study the wind speed impacts. As the well-known, the ambient winds may result in the deteriorated exhaust plume recirculation, thus bring on the increased inlet air temperature

of the ACCs. Figure 4 shows the inlet air temperatures of the axial flow fans at the wind speed of 9m/s and direction angle of 90°. The high inlet air temperatures for the upwind condenser cells are clearly observed for the ACCs without FGD. However with the configuration of the FGD, the inlet air temperatures for the upwind condenser cells are lowered. From the figures can also be seen that the small obliquity of the FGD is superior to the large obliquity for the inlet air temperatures of the upwind condenser cells. It shows that a lower FGD obliquity is favourable for the exhaust plume recirculation improvement of the ACCs.

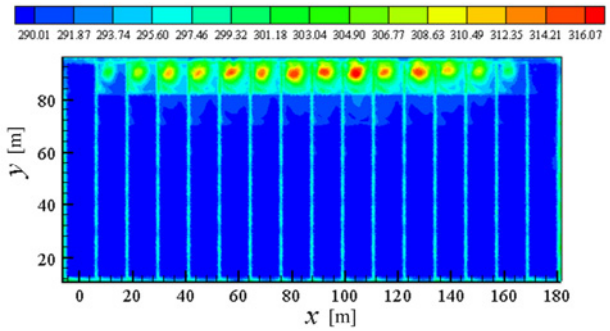

(a)

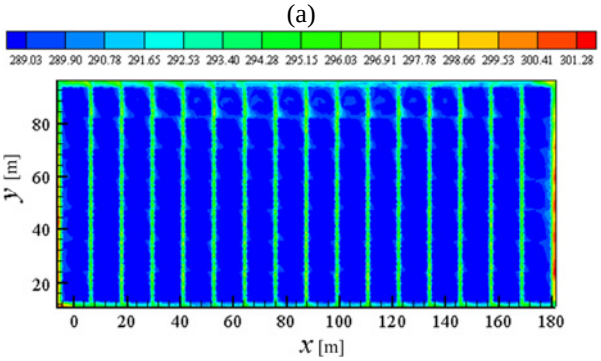

(b)

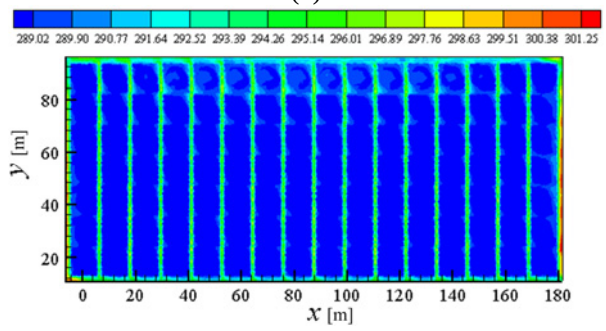

(c)

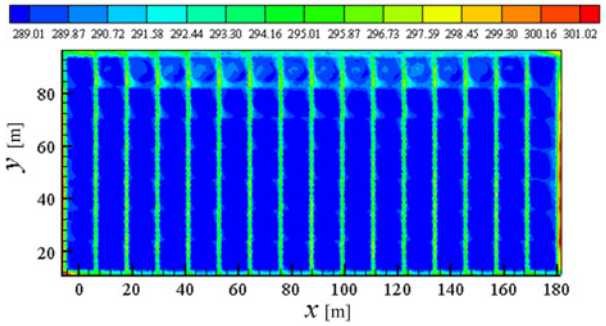

(d)

Figure 4 Temperature contours at the inlet of the axial flow fans at the wind speed of 9m/s and direction angle of 90°. (a) without FGD, (b) with FGD at slats obliquity of 30°, (c) with FGD at slats obliquity of 45°, (d) with FGD at slats obliquity of 60°.

The variations of the volumetric flow rate with the wind speeds and direction angles are shown in Figure 5. It can be seen that the volumetric flow rate always has a notable increase at any wind speeds and direction angles when the FGD is installed. It shows that the FGD can restrain the flow distortions at the fan inlet thus improve the fan performance. With the increase of the wind speed, the increase of the flow rate thanks to the flow field leading of the FGD becomes more conspicuous. The higher the wind speed, the better the improvement of the ACC flow performance by the FGD. Generally the obliquity of 30° is superior to the obliquity of 45° and 60° and the obliquity of 45° is superior to the obliquity of 60°. The lower obliquity is more beneficial to the fan performance. At the wind speed of 15m/s and direction angle of -90° as an illustration, the volumetric flow rate increases by 22.3% at the obliquity of 30°, 19.4% at the obliquity of 45°, 18.3% at the obliquity of 60°.

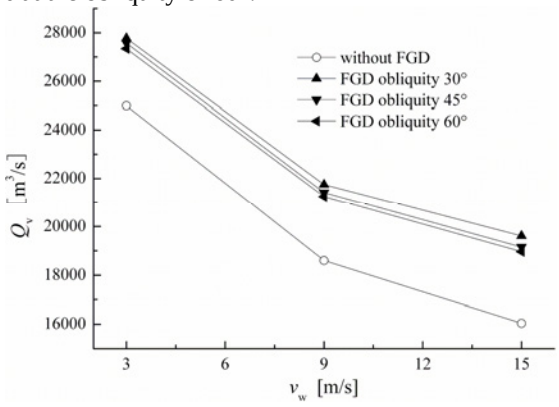

(a)

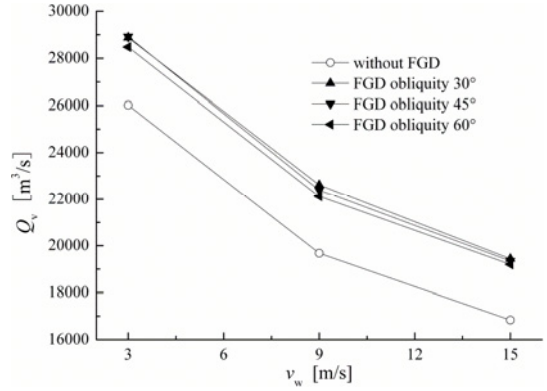

(b)

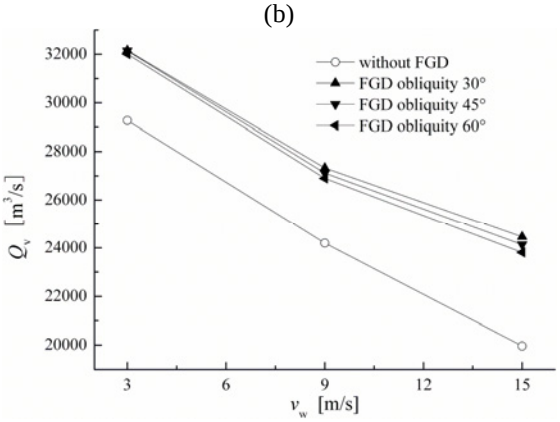

(c)

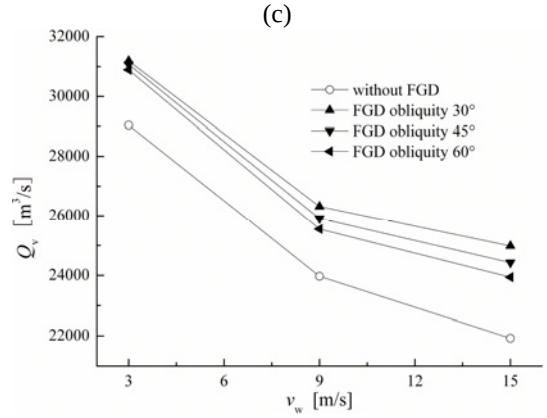

(d)

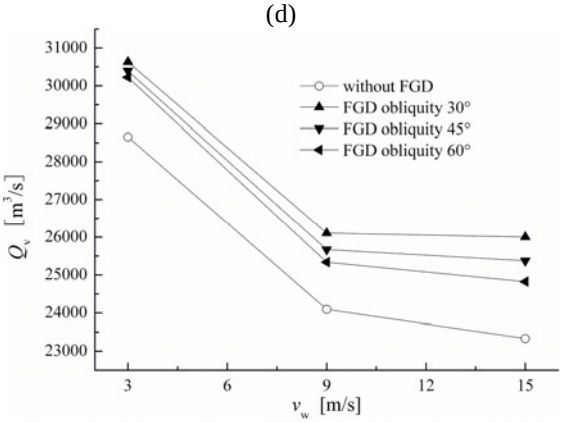

(e)

Figure 5 Average volumetric flow rate of the two ACCs versus wind speed at different FGD obliquities. (a) -90°, (b) -45°, (c) 0°, (d) 45°, (e) 90°.

Figure 6 shows the average heat rejection of the two ACCs versus the wind speeds and direction angles. Similar to the changing trends of the flow rate, the heat rejection also has a clear increase thanks to the flow field leading by the FGD. The lower FGD obliquity is beneficial to the heat transfer performance especially at the wind direction angle of 45° and 90°. At the wind speed of 15m/s and direction angle of 0° as an example, the heat rejection increases by 21.1% at the obliquity of 30°, 19.7% at the obliquity of 45°, 18% at the obliquity of 60°.

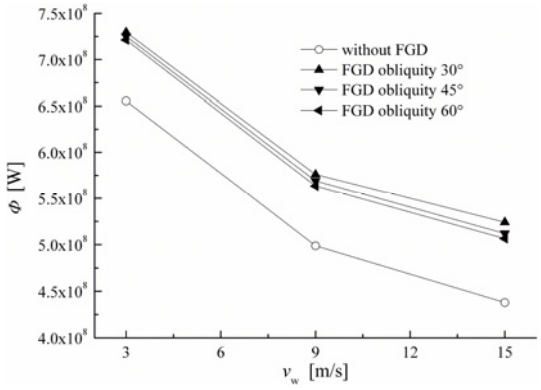

(a)

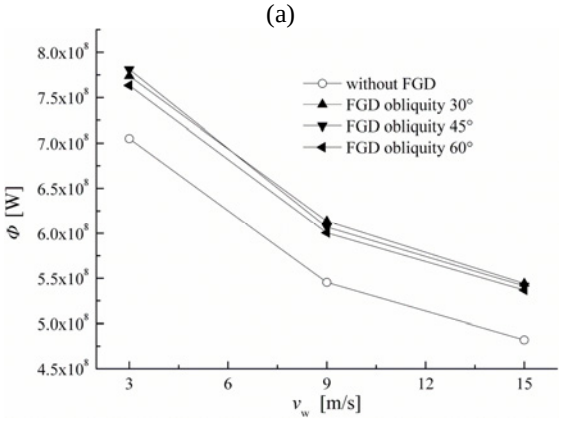

(b)

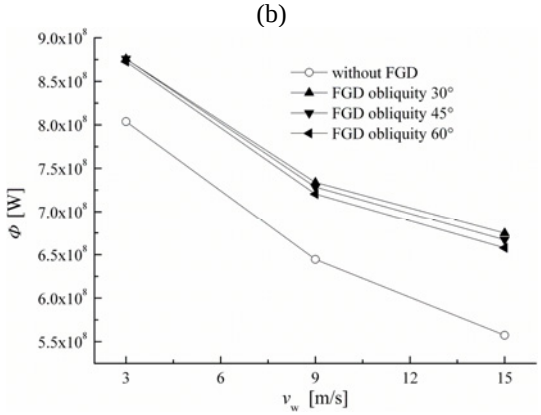

(c)

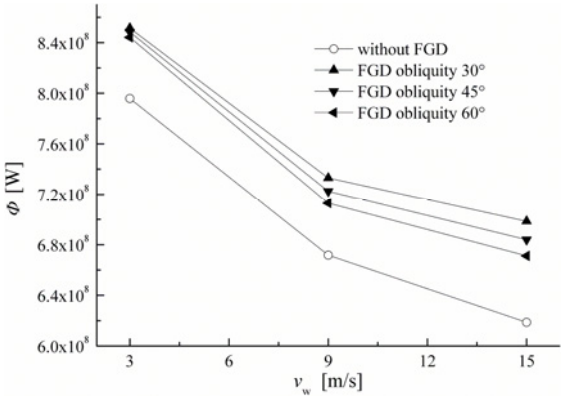

(d)

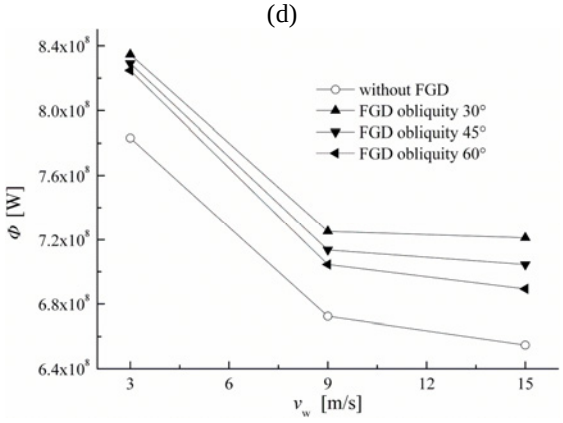

(e)

Figure 6 Average heat rejection of the two ACCs versus wind speed at different FGD obliquities. (a) -90°, (b) -45°, (c) 0°, (d) 45°, (e) 90°.

The thermo-flow characteristics of the condenser cells are also obtained. Figure 7, 8 and 9 show the volumetric flow rate and heat rejection of the condenser cells at the Row 1, 4 and 7 (leading edge, middle, trailing edge) respectively. The increases of both the volumetric flow rate and heat rejection thanks to the FGD are clearly found. For the upwind condenser cells at the Row 1, the increases are much more conspicuous. For the condenser cell at the Row 1 and column 6 as an example, the heat rejection increases by 271% at the obliquity of 30°, 221% at the obliquity of 45°, 163% at the obliquity of 60°. However for the condenser cell at the Row 7 and column 6, the heat rejection increases only by 3.4% at the obliquity of 30°, 3% at the obliquity of 45°, 2.9% at the obliquity of 60°. It shows that the flow field leading resulting from the FGD is much more favourable to the improvement of the thermo-flow performances of the upwind condenser cells.

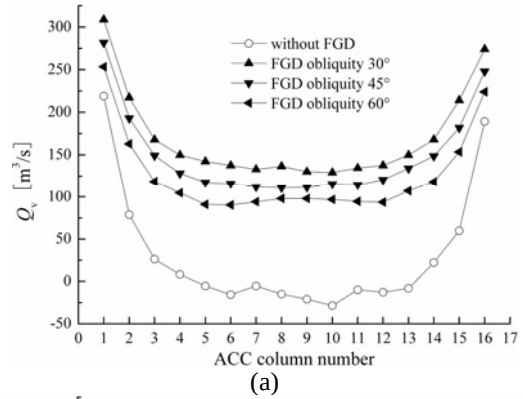

(a)

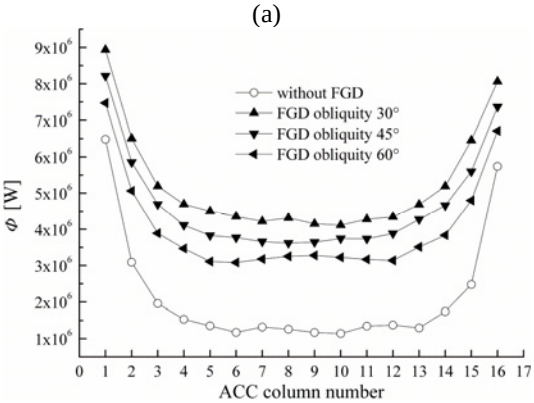

(b)

Figure 7 Volumetric flow rate and heat rejection of the Row 1condenser cells at the wind speed of 9m/s and direction angle of 90°. (a) volumetric flow rate, (b) heat rejection.

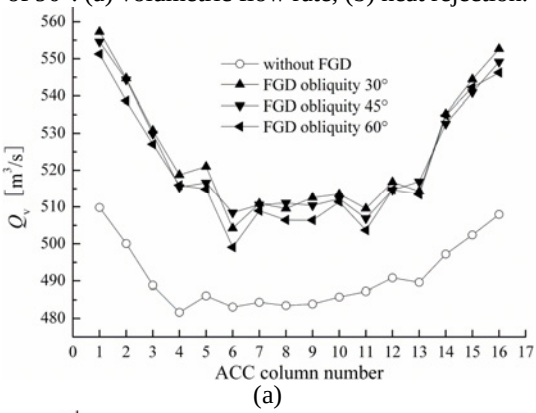

(a)

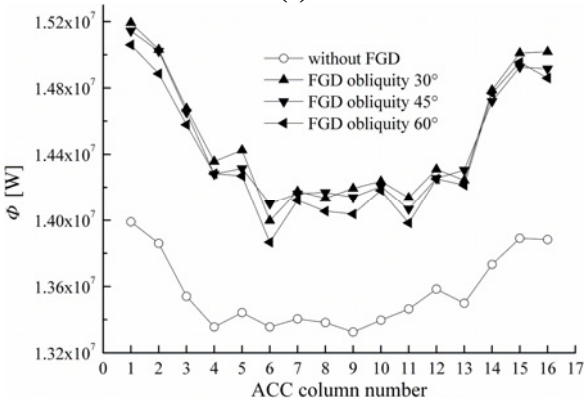

(b)

Figure 8 Volumetric flow rate and heat rejection of the Row 4 condenser cells at the wind speed of 9m/s and direction angle of 90°. (a) volumetric flow rate, (b) heat rejection.

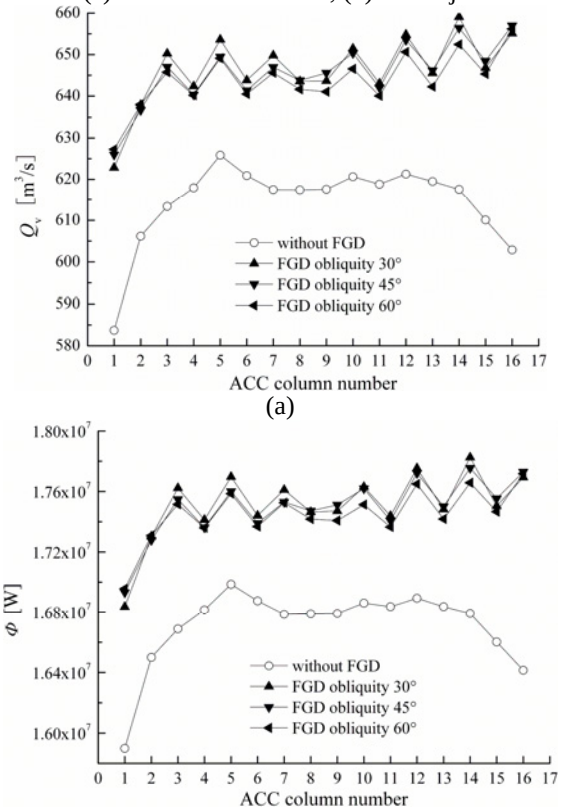

Figure 9 Volumetric flow rate and heat rejection of the Row 7condenser cells at the wind speed of 9m/s and direction angle of 90°. (a) volumetric flow rate, (b) heat rejection.

CONCLUSION

Three obliquities of the FGD are investigated to present the improvement of the thermo-flow characteristics of the whole ACCs and the condenser cells by the flow field leading from the FGD. The lowered inlet air temperatures of the axial flow fans show that the flow guiding device can restrain the exhaust plume recirculation and improve the heat transfer performances of the ACCs. Thanks to the weakened flow distortions at the inlet of the fan by the flow field leading, the volumetric flow rate of the ACCs has a notable increase especially for the upwind condenser cells. The heat rejection of the ACCs has the similar changing trends as the volumetric flow rate. The low obliquity of the FGD is superior to the high one for the improvement of the thermo-flow performances especially at the wind direction angle of 45° and 90°. It is of use for the optimal design and operation of the direct dry cooling system to investigate the effects of the FGD obliquities on the thermo-flow performances of the ACCs.

ACKNOWLEDGEMENT

This research is supported by the National Basic Research Program of China (973 Program) (Grant No. 2009CB219804) and National Key Technology R&D Program of China (Grant No. 2011BAA04B02).

REFERENCES

[1] Tawney, R., Khan, Z., and Zachary, J., Economic and Performance Evaluation of Heat Sink Options in Combined Cycle Applications, *ASME J. Eng. Gas Turbines Power*, Vol. 127, No. 2, 2005, pp. 397-403

[2] Wilber, K.R., and Zammit, K., Development of Procurement Guidelines for Air-cooled Condensers, Advanced Cooling Strategies/Technologies Conference, 2005, Sacramento, California, June 1-2

[3] Duvenhage, K., and Kroger, D.G., The influence of wind on the performance of forced draught Air-cooled heat exchangers, *J. Wind Eng. Ind. Aero.*, Vol. 62, No. 2-3, 1996, pp. 259-277

[4] van Rooyen, J.A., and Kroger, D.G., Performance trends of an Air-cooled steam condenser under windy conditions, *ASME J. Eng. Gas Turbines Power*, Vol. 130, No. 2, 2008, 023006

[5] Hotchkiss, P.J., Meyer, C.J., and von Backstrom, T.W., Numerical investigation into the effect of cross-flow on the performance of axial flow fans in forced draught Air-cooled heat exchangers, *Appl. Therm. Eng.*, Vol. 26, No. 2-3, 2006, pp. 200-208

[6] Meyer, C.J., Numerical investigation of the effect of inlet flow distortions on forced draught air-cooled heat exchanger performance, *Appl. Therm. Eng.*, Vol. 25, No. 11-12, 2005, pp. 1634-1649

[7] Duvenhage, K., Vermeulen, J.A., Meyer, C.J., and Kroger, D.G., Flow distortions at the fan inlet of forced-draught Air-cooled heat exchangers, *Appl. Therm. Eng.*, Vol. 16, No. 8-9, 1996, pp. 741-752

[8] Meyer, C.J., and Kroger, D.G., Plenum chamber flow losses in forced draught air-cooled heat exchangers, *Appl. Therm. Eng.*, Vol. 18, No. 9-10, 1998, pp. 875-893

[9] Meyer, C.J., and Kroger, D.G., Numerical investigation of the effect of fan performance on forced draught air-cooled heat exchanger plenum chamber aerodynamic behavior, *Appl. Therm. Eng.*, Vol. 24, No. 2-3, 2004, pp. 359-371

[10] Bredell, J.R., Kroger, D.G., and Thiart, G.D., Numerical investigation of fan performance in a forced draft Air-cooled steam condenser, *Appl. Therm. Eng.*, Vol. 26, No. 8-9, 2006, pp. 846-852

[11] Gu, Z.F., Chen, X., and Lubitz, W., Wind tunnel simulation of exhaust recirculation in an Air-cooling system at a large power plant, *Int. J. Therm. Sci.*, Vol. 46, No. 3, 2007, pp. 308-317

[12] Yang, L.J., Du, X.Z., and Yang, Y.P., Measures against the adverse impact of natural wind on Air-cooled condensers in power plant, *Sci. China Tech. Sci.*, Vol. 53, No. 5, 2010, pp. 1320-1327

[13] Wei, J.J., Zhang, C.W., Gao, X.F., and Yu, B., Performance Predication of an Improved Air-cooled Steam Condenser with Deflector under Strong Wind, 2nd Asian Symposium on Computational Heat transfer and Fluid Flow, Proceedings of ASCHT 09, 2009, paper no. ASCHT 2009-C55

[14] Owen, M.T.F., and Kroger, D.G., The effect of screens on air-cooled steam condenser performance under windy conditions, *Appl. Therm. Eng.*, Vol. 30, No. 16, 2010, pp. 2610-2615